UNIVERSITY OF TARTU
Faculty of Science and Technology
Institute of Technology

Anjali Gyawali

Characterization of Human MAGE-A10 protein

Bachelor's Thesis (12 ECTS)

Curriculum Science and Technology

Supervisor:
MSc Anneli Samel

Tartu 2022

ACKNOWLEDGEMENTS

I would first like to express my appreciation and thank my supervisor Anneli Samel for her immense support, guidance, encouragement, and patience throughout my thesis. Thank you very much for the support and help with your scientific and technical ideas. You have been an excellent mentor to me. Also, many thanks to Eve for helping me with confocal microscopy.

I am grateful and owe my thanks to Professor Reet Kurg for giving me an opportunity to work in her lab with her amazing and highly motivated groups. I appreciate your tremendous encouragement, motivation, and valuable suggestions when required. You supported me academically and emotionally and helped me focus on my paths when I required it the most. Thank you very much. I would like to express my gratitude to all my Bioengineering and Robotics colleagues.

Last but not least, my special thanks to my parents (Tikaram and Bhagwati) and my brothers (Asim and Jeevan Gyawali), whose support, guidance, and relentless encouragement have given me immense support and strength during my academic studies to achieve my goal.

Characterization of Human MAGE-A10 protein

Abstract:

MAGE-A10, the most antigenic protein member of the MAGE-A family of cancer-testis antigen (CTAs), is expressed in tumors but not in normal tissues except for the testis, fetal ovary, and placenta. Their tumor-restricted expression pattern makes these proteins an attractive target for cancer immunotherapy. The computational molecular weight of MAGE-A10 is ~41kDa. However, in the gel, it runs at ~72kDa. In this research, COP5-EBNA cells were transfected with plasmid DNA encoding for different stretches of the MAGE-A10 protein, and the size anomalies and localization of the proteins were determined. Our results suggested that the N-terminal region of the protein is responsible for the size anomalies and nuclear localization of the MAGE-A10 protein.

Keywords:

MAGE-A10, MAGE-A, cancer-testis antigen, testis, cancer immunotherapy

CERCS:

T490 Biotechnology, P310 Proteins, enzymology

Inimese MAGE-A10 valgu iseloomustamine

Lühikokkuvõte:

MAGE-A vähi-testise antigeenide (VTA) perekonna kõige antigeensem liige MAGE-A10 ekspresseerub vähkkudedes, kuid puudub enamikes normaalkudedes, erandiks testised, loote munasarjad ning platsenta. Selline vähispetsiifiline avaldumismuster teeb sellest valgust hea sihtmärgi vähi immuunteraapias. MAGE-A10 valgu arvutuslik suurus on umbes 41kDa, kuid valgugeelis paistab selle suurus olevat 72kDa. Selles uurimuses transfekteeriti COP5-EBNA rakke MAGE-A10 eri lõike kodeerivate plasmiidsete DNA-dega ning uuriti toodetud valkude suurust ja lokalisatsiooni rakkudes. Saadud tulemustest nähtub, et arvutusliku ja tegeliku suuruse erinevuste ning tuumalokalisatsiooni eest vastutab valgu N-terminaalne regioon.

Võtmesõnad:

MAGE-A10, MAGE-A, vähi-testise antigeen, testis, vähi immuunteraapia

CERCS:

T490 Biotehnoloogia, P310 Valgud, ensümoloogia

TABLE OF CONTENTS

TERMS, ABBREVIATIONS, AND NOTATIONS

AMPK – adenosine monophosphate-activated protein kinase

BSA –bovine serum albumin

CTAs – cancer testis antigens

CTL – cytotoxic T-lymphocytes

DAPI – 6-diamidino-2-phenylindole

ECL – electrochemiluminescence

EDTA – ethylenediamineetetraacetic acid

FCS – fetal calf serum

GAGE – G antigen

HDAC – histone deacetylases

HRP – horseradish peroxidase

IMDM – Iscove's Modified Dulbecco's Media

KAP1 – krüppel-associated box domain-associated protein-1

KRAB – krüppel-associated box

KZNF – KRAB zinc-finger proteins

MAGE – melanoma antigen genes

MAGE-A – melanoma antigen gene A

MAGE-A10 – melanoma antigen gene A10

MHD – melanoma antigen gene homology domain

NFDM – non-fat dry milk

NLS – nuclear localization signal

PAGE – polyacrylamide gel electrophoresis

PBS – phosphate-buffered saline

PFA – paraformaldehyde

pQM-MAGE-A10 – MAGE-A10 plasmid

PTMs - post-translational modifications

PVDF – polyvinylidene fluoride

RING – really interesting new gene

SDS – sodium dodecyl sulphate

SKIP – Ski-interacting protein

TRIM28 – tripartite motif-containing 28

TRIM31 – tripartite motif-containing 31

XAGE – X chromosome antigen

INTRODUCTION

Cancer-testis antigens have been in the centre of cancer immunotherapy research for a few decades, since they have a very unique expression pattern along with high immunogenicity which allows for very precise cancer cell targeting in both diagnostics and treatment. One of the families that have been studied widely, is the MAGE family, more precisely MAGE-A, since members of this family of CTAs are highly immunogenic and might play a significant role in the formation on metastases.

Previous studies have found MAGE-A10 to be one of the most immunogenic members of the MAGE-A family and therefore an extremely attractive target for cancer immunotherapy and/or vaccines. However, since fundamental knowledge about this particular protein has some gaps, further investigation was needed to help future clinical trials succeed.

This study aims to characterize the human MAGE-A10 protein beyond what is known. Firstly, the aim is to discover which stretch of amino acids acts as a nuclear localization signal. Secondly, since the protein should computationally only be around 41kDa in size, compared to the previously described 72kDa, this study aims to determine which stretch/stretches of amino acids are responsible for this size anomaly.

1 LITERATURE REVIEW

1.1 Cancer

According to WHO (World Health Organization, 2006), more than 11 million people are diagnosed with cancer each year, causing a mortality rate of 12.5% worldwide (Gonzaga Almeida et al., 2009). As of 2020, cancer accounts for nearly 10 million deaths annually (World Health Organization, 2022). It is a highly prevalent group of diseases that can affect any part of the body, invading the adjoining parts and spreading to other organs in the body, forming metastasis. These widespread metastases are the main factor in causing death in cancer (World Health Organization, 2022).

Cancer is one of the leading causes of death worldwide, and this increase in cancer-related mortality raises the urgent need for cancer treatment (Gonzaga Almeida et al., 2009). One approach is immunotherapy which has not yet been thoroughly studied (Gonzaga Almeida et al., 2009). Immune therapy uses the body's immune system to treat cancer, making it a better alternative to conventional treatments such as chemotherapy and radiation, which are often ineffective against some cancers, like melanoma (Cancer Research Institute, 2022b). Clinical studies have shown that immunotherapy is more durable and allows long-term cancer remission (Cancer Research Institute, 2022b). In fact, it can direct the immune system to remember cancer cells even after the treatment has been completed (Cancer Research Institute, 2022b). Immunotherapy might not have adverse side effects like those of chemotherapy and radiation, which affect cancer cells as well as healthy cells resulting in hair loss and nausea (Cancer Research Institute, 2022b).

In contrast, immunotherapy is more targeted, making it a better alternative than other treatments and a critical field of research and study (Cancer Research Institute, 2022b). Different approaches to cancer immunotherapy are used to treat cancers, such as Adoptive Cell Therapy, Cancer vaccines/Therapeutic vaccines, Immunomodulators, and Oncolytic virus therapy (Cancer Research Institute, 2022a). Therapeutic cancer vaccines are one approach to immunotherapy that explicitly targets and regulates cellular immune responses to identify and destroy cancer cells based on specific antigens such as cancer-testis antigens (CTAs) expressed primarily in tumors (Gonzaga Almeida et al., 2009).

1.2 Cancer testis antigens

Cancer-testis (C.T.) genes are diverse genes expressed predominantly in normal testicular tissues and various human cancers (Kulkarni et al., 2017). Cancer-testis (C.T.) genes were named Cancer-testis antigens (CTAs) because they can encode immunogenic antigens that lead to immune responses in cancer patients (Chang et al., 2019). Hence, cancer-testis antigens are studied as a potential target for cancer immunotherapy due to their significant properties, i.e., their stable and specific expression in tumor cells and lack of expression in normal tissues (Taguchi et al., 2014).

According to Lira Da Silva, 745 putative cancer-testis antigen genes have been identified (Lira Da Silva et al., 2017). They are broadly divided into CT-X antigens located on the X-chromosome and non-X CTAs located on numerous autosomes (Kulkarni et al., 2017). The genes located on the X-chromosome form multigene families that share a common genomic locus, examples of these are melanoma antigen gene (MAGE), G antigen (GAGE), and X-chromosome antigen (XAGE) (Doyle et al., 2010).

1.3 MAGE family

Thierry Boon and colleagues cloned the first human tumor antigen from melanoma patient cells using the melanoma cell line MZ2-MEL and autologous CTL (cytotoxic T-lymphocytes) clones cytolytic to melanoma antigen (MAGE)-1 (van der Bruggen et al., 1991). MAGE-1 belongs to a more prominent family of genes known as MAGEs that comprises 38 genes and 18 pseudogenes annotated in humans (van der Bruggen et al., 1991). Since then, in 2001, 22 more genes were added to this gene family based on their sequence similarity, i.e., 60 genes in total, including pseudogenes (Chomez et al., 2001). The Melanoma Antigen Genes (MAGE) were classified as cancer-associated antigens and are therefore intriguing targets to be used as biomarkers or for immunotherapy against cancer because subclasses of these >40 human proteins are expressed in a variety of cancers, whereas their expression in normal tissues is mainly limited to the testis and in some cases ovarian and placental tissues (Y. Liu et al., 2019).

MAGE genes are conserved in all eukaryotes, with the gene copy number increasing rapidly in mammals (S. Liu et al., 2020). Based on the tissue expression pattern and gene structure, human MAGE family members are classified into Type I MAGEs and Type II MAGEs (**Figure 1**) (van der Bruggen et al., 1991). Type I MAGEs, which are more prominent in number and classified as cancer-testis antigens (CTAs), include the MAGE-A, MAGE-B, and

MAGE-C subfamilies **(Figure 1)** located on the X-chromosome (de Donato et al., 2017). These Type I MAGEs are highly expressed in testis and cancer cells and include nearly 45 genes, including 12 MAGE-A, 18 MAGE-B, and 7 MAGE-C genes (Chomez et al., 2001).

The Type II MAGE genes classified as ubiquitous MAGEs (Barker & Salehi, 2002a) are distributed in various locations in the genome, have heterogeneous structures with no relation to cancer, and are expressed in multiple normal tissues in the body (Töhönen et al., 2000). The family of Type II MAGEs has been expanded to MAGE-D1/NRAGE/Dlxin-1, MAGE-D2, MAGED3/Trophinin/Magphinin, MAGE-E1/MAGE-D4, MAGEE2, MAGE-F1, MAGE-G1/Necdin-like 2, MAGE-H1, MAGE-L2, and Necdin (**Figure 1**) (Y. Liu et al., 2012). The genes that form the Type II MAGE family play a vital role in the organism due to their functions in cell differentiation and regulation of cell cycle progression (de Donato et al., 2017). Also, MAGEs might function in the ubiquitination cascade mediated by RING proteins as they act as a binding partner for both Type I and Type II MAGE proteins (Yang et al., 2007).

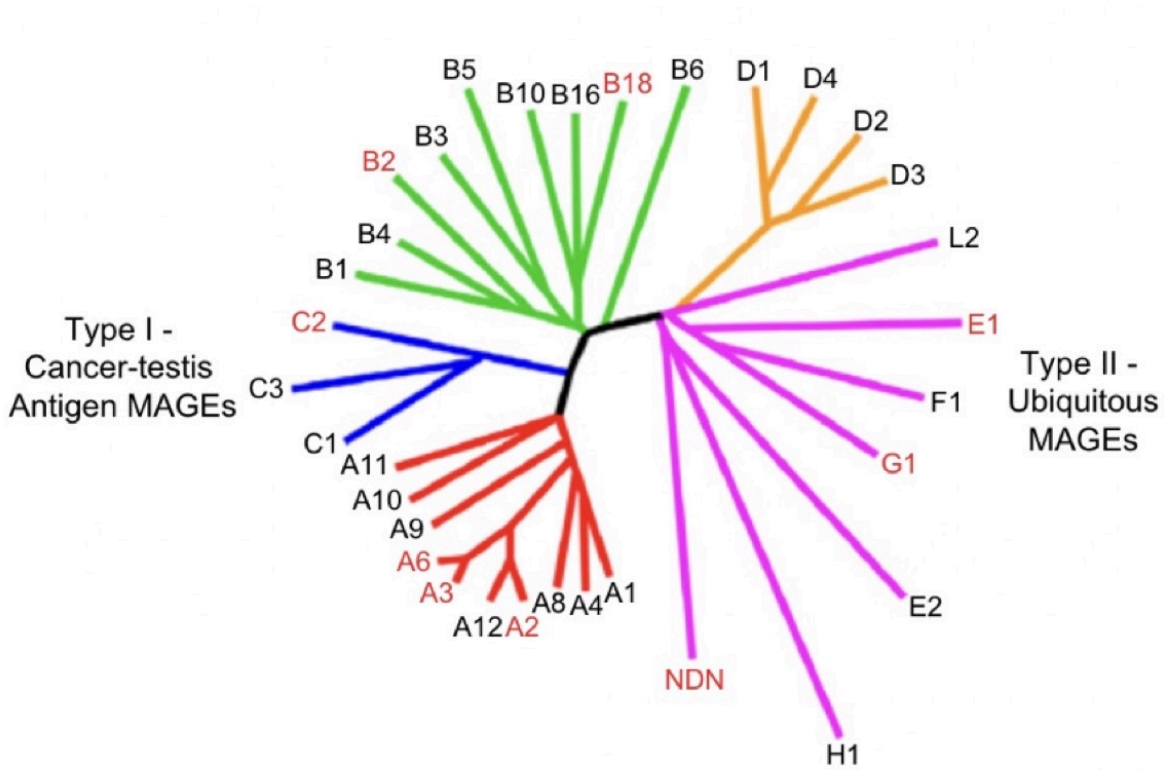

Figure 1. Sub-Classes of MAGE Family. Dendrogram tree of the MAGE family. The MAGE family is divided into Type I and Type II. Type I is only expressed in testicular and placental tissues in normal tissues and at different levels in numerous tumors. Type I MAGEs include MAGE-A, MAGE-B, and MAGE-C families. Type II MAGEs are expressed in various normal tissues. Type II MAGEs include MAGE-D, MAGE-E, MAGE-F, MAGE-G, MAGE-H, MAGE-L2, and Necdin families (Doyle et al., 2010).

1.4 MAGE homology domain

Both Type I and Type II MAGE proteins share a conserved domain known as the MAGE homology domain (MHD) (**Figure 2**) (Doyle et al., 2010). The MAGE homology domain (MHD) was originated from protozoa and is approximately 170 amino acids long (López-Sánchez et al., 2007). All human MHDs are 46% conserved (Doyle et al., 2010; Weon & Potts, 2015)**.** In contrast, MHDs within specific sub-families are even more conserved. For example, the four MAGE-D MHDs are up to 75% conserved, and between the twelve MAGE-A genes, the MHDs are 70% conserved (Doyle et al., 2010). This high conservation of the MHDs among the sub-families shows that MAGE proteins may share a similar function and structure that might contribute to their physiology and cancer development (Meek & Marcar, 2012). Despite MHDs sharing structural similarities and being conserved between the two types, the biochemical function of the MAGE homology domain (MHD) is still complex to understand (Doyle et al., 2010).

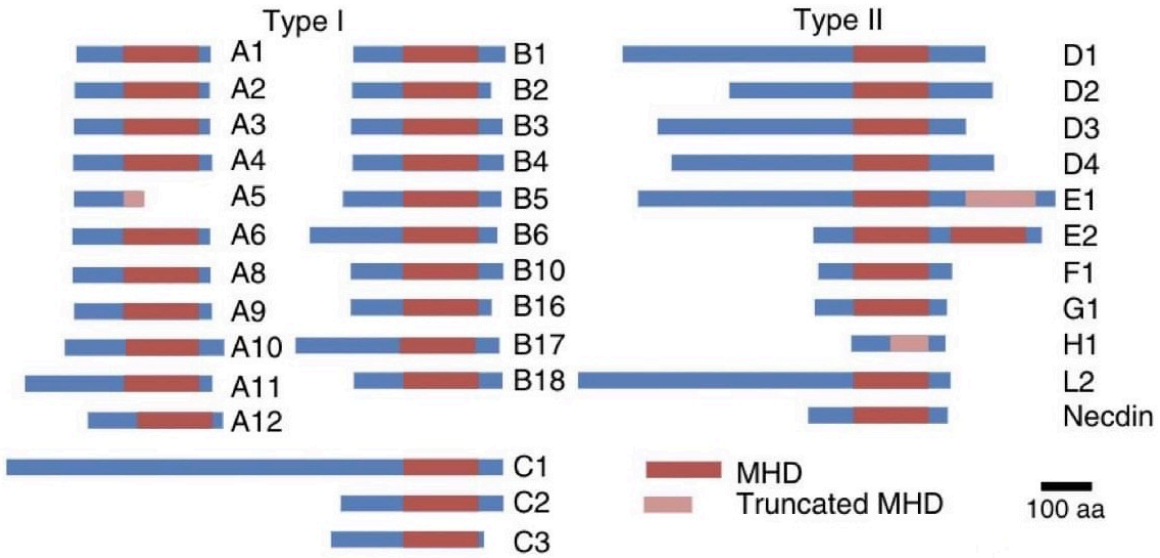

Figure 2. The MAGE homology domain. List of human MAGE proteins and their conserved MAGE homology domain (MHD) highlighted in maroon. Some MAGEs have truncated MHDs, such as MAGE-A5 in Type I (Weon & Potts, 2015).

1.5 MAGE-A genes

MAGE-A genes located on the X-chromosome (de Plaen et al., 1994) encode for human tumor antigens that are identified by autologous cytolytic T lymphocytes (CTLs) using various HLA molecules (van der Bruggen et al., 1991). MAGE-A genes are expressed by numerous human cancers such as melanoma, breast cancer, bladder cancer, and lung cancer but are silenced in normal adult tissues except the testis and, in some cases, placenta (de Plaen et al., 1994). Recent studies have shown that MAGE-A genes are also exclusively expressed in the bone marrow (Colemon et al., 2020). As MAGE-A expression is related to tumor malignancy and is mainly confined to cancer tissues, their tumor-associated peptides (van der Bruggen et al., 1991) could be a significant target for cancer vaccine development (Atanackovic et al., 2004).

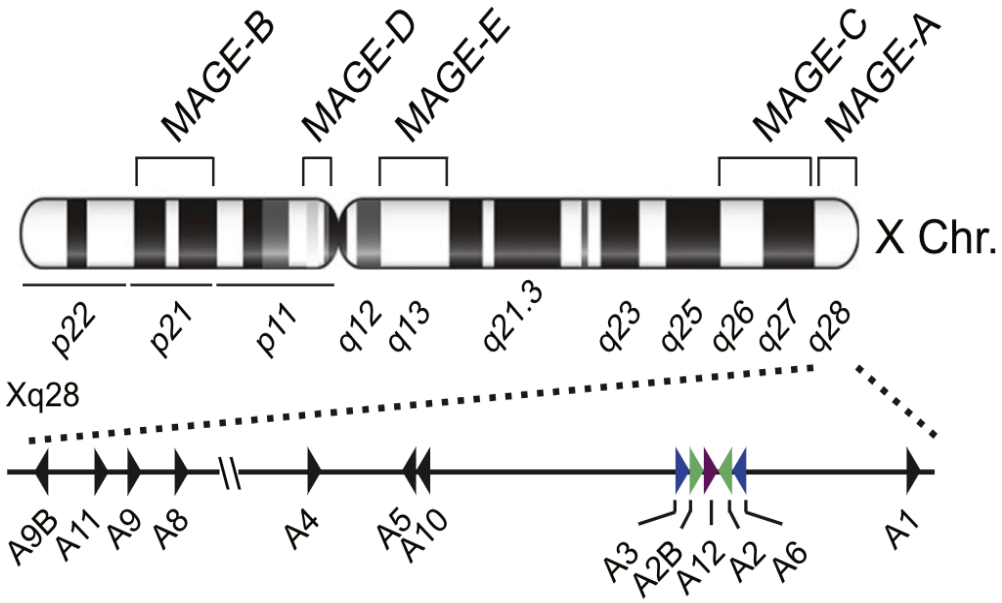

Figure 3. **Chromosomal Organization of MAGE Sub-families on the X-chromosome**. The MAGE-A genes are located in the q28 region of the X-chromosome. The Black triangles represent the gene orientation. The colored triangles represent the palindrome arrangement of the MAGE-A genes (Lee & Potts, 2017).

The MAGE-A gene family consists of 12 homologous genes, namely MAGE-A1 to MAGE-A12 (van der Bruggen et al., 1991), which are all clustered in the Xq28 region (**Figure 3)** (de Plaen et al., 1994; Rogner et al., 1995). Alongside MAGE-A genes, the X-chromosome also contains other MAGEs, both Type I and Type II (Muscatelli et al., 1995; Rogner et al., 1995). Type I includes six MAGE-B genes located in Xp21 and three MAGE-C genes located in Xq26-27 (Muscatelli et al., 1995; Rogner et al., 1995). Type II includes the MAGE-D subfamily constituting four genes located in Xp11 and the three MAGE-E genes located in Xq13 (Lucas et al., 1998). However, most Type II MAGEs are not clustered on the X-chromosome as they are single-copy genes (Lucas et al., 1998). All in all, the X-chromosome contains large, homologous inverted repeats predominantly expressed in the testis (Warburton et al., 2004).

Type I MAGEs contain 3 or 4 exons (Forslund & Nordqvist, 2001; Lee & Potts, 2017), with the ORF located within the terminal exons (Muscatelli et al., 1995). A single exon characterizes Type II MAGEs; however, MAGE-D genes have a different gene structure, i.e., each MAGE-D gene consists of 13 exons, with the ORF being split over 11 exons (Lee & Potts, 2017).

1.5.1 Expression pattern of MAGE-A genes

mRNA expression analysis revealed that MAGE-A genes are expressed in testicular tissue and not in other normal cells or somatic tissues, including melanocytes (Caballero & Chen, 2009). In contrast, these genes show their expression in different types of human cancers, such as lung cancer, breast cancer, ovarian cancer, and bladder cancer (Rimoldi et al., 1999). According to Becker, MAGE-A1 showed expression in the skin during wound healing (Becker et al., 1994). Among the various members of the MAGE family, analysis of different tissues disclosed that MAGE-A1, A2, A3, A4, A6, and A12 are highly expressed in tumor tissues and cancerous cell lines showing no expression in normal adult tissues except for testis and that MAGE-A3, A4, A8, A9, A10, and A11 are also expressed in placenta (de Plaen et al., 1994). MAGE-A7 was found to be silent in various tissues, including the testis, and confirmed to be a pseudogene that is not transcribed (Chomez et al., 2001). Antibodies against MAGE recombinant proteins were produced to study the expression pattern of MAGE genes at the protein level (Rimoldi et al., 1999). Concurrent analyses have shown that MAGE-A1, A2, A3, A4, A5, A6, A8, A9, A10, A11, and A12 are expressed at a protein level (Meek & Marcar, 2012).

1.6 MAGE-A proteins

MAGE-A protein lengths range from 124 to 419 amino acid residues (Meek & Marcar, 2012). The MAGE-A1 protein was shown to be 57%-77% identical to MAGE-A2, A3, A4, A6, and A8, A9, A10, A11, and A12 proteins, whereas a PCR assay confirmed that MAGE-A3 and MAGE-A6 were 99% identical to each other (de Plaen et al., 1994). The molecular weight of MAGE-A1, A3, A4, and A11 proteins is estimated to be between 45- to 50 kDa (Jurk et al., 1998; Shichijo et al., 1995), whereas MAGE-A10 appears to be 72 kDa (Rimoldi et al., 1999).

1.7 Functions of MAGE-A proteins

Different types of cancer with high tumorigenicity and specificity have shown overexpression of MAGE-A proteins (P. Yang et al., 2021). MAGE-A proteins can regulate different transcriptional events, for example, integration of the co-repressor, KAP1(krüppel-associated box domain-associated protein-1) (also known as TRIM28 (tripartite motif-containing 28)) to KRAB (krüppel-associated box) domain zinc-finger KZNF (KRAB zinc-finger proteins) transcription factors by MAGE-A3 (Doyle et al., 2010; Xiao et al., 2011; B. Yang et al., 2007). Numerous MAGE-A proteins show their involvement in regulating transcription, mainly in cancer-associated pathways (Laduron et al., 2004). For example, MAGE-A1 can act as a repressor that binds to SKIP (SKI-interacting protein) and recruits HDAC (histone deacetylases) proteins, by which it can interrupt NOTCH1-mediated signal transduction (Laduron et al., 2004). In addition to these, MAGE-A2 could interact and repress the p53 activity by recruiting transcription repressors (HDACs) to p53 transcription sites (Monte et al., 2006). Studies have shown that Type I and Type II MAGE proteins promote ubiquitination by acting as activators of RING (really interesting new gene) E3 ubiquitin ligases (Doyle et al., 2010; B. Yang et al., 2007).

1.7.1 Enhancing E3 RING ubiquitin ligase activity

Studies have shown that MAGEs interact with other proteins, especially E3 ubiquitin ligases (Weon & Potts, 2015). Ubiquitination refers to the covalent post-translational modifications (PTMs) of lysine residues on substrate proteins, regulating almost all aspects of cell functions (Lee & Potts, 2017). Growing research has shown that MAGE binding can enhance TRIM28 (also referred to as KAP1) ubiquitin ligase activity against p53, resulting in the degradation of the protein in a proteasome development order (Doyle et al., 2010; Weon &

Potts, 2015). Most of the known E3 ubiquitin ligases contain the RING domain, which catalyzes substrate recognition and ubiquitin ligation by activating the E2 enzyme (Lorick et al., 1999). Hence, it has been unveiled that many RING ligases were implicated in cancer because of their role in cellular homeostasis and genomic integrity (Lipkowitz & Weissman, 2011). MAGEs form complexes with E3 RING ubiquitin ligases that were identified from the direct binding of MAGE-A2, MAGE-A3, MAGE-A6, and MAGE-C2 protein. MAGE proteins have been found to regulate TRIM28/KAP1 E3 ubiquitin ligase, a multifunctional protein involved in transcriptional regulation, DNA damage repair, and cellular differentiation (Doyle et al., 2010). For example, MAGE-A3 and the highly similar protein MAGE-A6 bind TRIM28 and enhance the ubiquitination of AMPKα1 (adenosine monophosphate-activated protein kinase) (Pineda et al., 2015). Interestingly, it has been reported that MAGE-A1 regulates not only TRIM28 ligase but also stimulates TRIM31 (tripartite motif-containing 31) ligase activity (Kozakova et al., 2015)

1.8 Immunological properties of MAGE-A proteins

Growing research and studies have shown that MAGE-A proteins serve as prognostic biomarkers due to their antigenic properties and as attractive immunotherapeutic targets due to their restricted expressions pattern (Makise et al., 2016). This restrictive expression of MAGE-A might make them less susceptible to tissue-specific immune tolerance while making it much easier to produce a robust immune response against MAGE-A (Duperret et al., 2018). Clinical studies have shown that MAGE-A targeted immunotherapy is effective in various cancer types (Saito et al., 2014; Vansteenkiste et al., 2013). Recent studies have revealed that compared to patients with lower or negative expression of MAGE-A, patients with esophageal, stomach, or lung cancer who expressed a higher level of MAGE-A were more susceptible to MAGE-A-targeted immunotherapies (Saito et al., 2014).

1.9 MAGE-A10

MAGE-A10 is the most antigenic protein member of the cancer-testis antigen (CTAs) family (Schultz-Thater et al., 2010). According to Carrel, the monoclonal antibodies against recombinant-MAGE-A1 protein identified a cross-reacting 72kDa antigen co-expressed with MAGE-A1 in melanoma cells (Carrel et al., 1996). This antigen was MAGE-A10 (Schultz-Thater et al., 2010), having a length of 369 amino acids (Meek & Marcar, 2012). According to the amino acid sequence, the computational molecular weight of MAGE-A10 protein is 41kDa (Barker & Salehi, 2002). However, while running in the gel, MAGE-A10 protein

appears to be larger than other members of the MAGE-A family. While most members of the MAGE-A have a molecular weight of 45-50 kDa, MAGE-A10 runs at 72kDa in the gel (Rimoldi et al., 1999). The reasons for this property of MAGE-A10 protein are still unknown. The MAGE-A10 gene consists of four exons and has a longer 3'-untranslated region, making its cDNA 0.7 kb more prolonged than those of other members of the MAGE-A family (Rimoldi et al., 1999).

According to Schultz-Thater, testis samples stained with GA11.1 monoclonal antibody were used to study the intracellular location of MAGE-A10 protein; this study revealed that the protein was expressed in spermatogonia and spermatocyte nuclei (Carrel et al., 1996). More than 50% of tumor cells express MAGE-A10 protein (Schultz-Thater et al., 2010). MAGE-A10 was detected in various cancers, including lung cancers, squamous cell carcinomas, adenocarcinomas, large and small cell cancers, and skin malignancies (Schultz-Thater et al., 2010). In addition to this, the protein was also detected in stomach cancers of the "intestinal-type" (Suzuki et al., 2008).

2 THE AIMS OF THE THESIS

- Determining the stretch of amino acid residues responsible for the size discrepancy of MAGE-A10.
- Determining the stretch of amino acid residues responsible for the nuclear localization of MAGE-A10.

3 EXPERIMENTAL PART

3.1 MATERIALS AND METHODS

3.1.1 Cell culture

The experiments were carried out in COP5-EBNA cells, a mouse fibroblast cell line produced in-house (described in Kurg et al., 2016). The cells were cultured in Iscove's Modified Dulbecco's Medium (IMDM), which contained 10% fetal calf serum (FCS), 100 U/ml penicillin, and 100 μg/ml streptomycin (Gibco, Thermo Fisher Scientific). The cells were incubated at 37º C in 5% CO2 using Galaxy® CO2 Incubator (Panasonic Healthcare Co; Ltd, Japan).

3.1.2 Plasmids

MAGE-A proteins were expressed in COP5-EBNA cells using in-house pQM plasmids obtained from Anneli Samel at the Institute of Technology (University of Tartu, Estonia). The gene segments were amplified with PCR (Polymerase Chain Reaction) and then cloned into the pQM vector containing the EGFP sequence in the C-terminus (Icosagen). E. coli (Escherichia coli) strain XL10 was used to propagate the plasmids. Transformed bacterial cells were grown in L.B. (Liquid Broth) medium with carbenicillin antibiotic (Gibco™). Then, the plasmids were isolated from bacterial cells with the NucleoBond® Xtra Midi E.F. (Macherey-Nagel) according to the manufacturer's protocol. Plasmids were used to express MAGE-A coding sequences fused in-frame with EGFP in the C-terminus.

3.1.3 Cell transfection

The electroporation method was used to transfect the plasmids into the COP5-EBNA cells. The cells were grown in 100 mm cell culture dishes until they reached ~90 % confluence. The medium was aspirated, and the cells were washed with 2-3 ml PBS (phosphate-buffered saline). The cells were then removed from the dish with 2ml of trypsin solution (0.05% trypsin, 0.02% EDTA (ethylenediamineetetraacetic acid) in PBS, G.E. healthcare) and transferred to a centrifuge tube with an equal volume of IMDM medium. The cells were centrifuged at 1000 rpm at 20ºC for 5 minutes (Eppendorf® centrifuge 5810R). The obtained supernatant was aspirated, and 250 μl of medium per electroporation was added to the cells. 5 μl of salmon sperm carrier DNA and 1 μg of the needed expression vector DNA were mixed with 250 μl of cell suspension and transfected by electroporation in 4-mm cuvettes

(Molecular Bioproducts) using GenePulser Xcell™ (Bio-Rad) at a capacitance of 975 μF and voltage of 230V. Then, the cells were transferred to a 15 ml centrifuge tube containing 3 ml of IMDM medium and centrifuged at 1000 rpm for 5 minutes at 20ºC (Eppendorf® centrifuge 5810R). The supernatant was aspirated, and the cells were resuspended in 1 ml of IMDM medium, then transferred onto a cell culture dish with media (8 ml of media per 100 mm dish) and grown for 24 hours at 37ºC in 5% CO2 using Galaxy® CO2 Incubator (Panasonic Healthcare Co; Ltd, Japan).

3.1.4 Antibodies

Both commercial and in-house antibodies prepared at the Institute of Technology of the University of Tartu (Tartu, Estonia) were used. The list of primary and secondary antibodies used in the experiment is shown in the tables below (**Table 1, Table 2**).

Table 1: List of primary antibodies used in the experiment.

Primary antibodies				
Antibodies	Initial Concentration	Western blot concentration	Immunofluorescence concentration	Manufacturer
anti-MAGE-A10 Polyclonal (mouse)	1.1 mg/ml	1:10,000	–	Institute of Technology, University of Tartu, Tartu, Estonia
anti-alfa-tubulin Monoclonal (mouse)	–	1:10,000	–	Sigma-Aldrich, St. Louis, MO, USA.
anti-GFP (mouse)	–	1:10,000	–	Institute of Technology, University of Tartu, Tartu, Estonia
anti-MAGE-A10 1D12 Monoclonal (mouse)	0.41 mg/ml	–	5 μg/ml	Kristina kurg, Institute of Technology, University of Tartu, Tartu, Estonia
anti-MAGE-A10 4B9 Monoclonal (mouse)	0.41 mg/ml	–	5 μg/ml	Kristina kurg, Institute of Technology, University of Tartu, Tartu, Estonia

Table 2: List of secondary antibodies used in the experiment.

Secondary antibodies				
Antibodies	Initial concentration	Western blot concentration	Immunofluorescence concentration	Manufacturer
goat-anti-rabbit	0.8 mg/ml	1:10,000	–	Invitrogen, Thermo Fisher Scientific, USA
goat-anti-mouse	–	1:10,000	–	Invitrogen, Thermo Fisher Scientific, USA
anti-mouse Alexa Fluor 568	1 mg/ml	–	1:1000	Invitrogen, Thermo Fisher Scientific, USA

3.1.5 Flow Cytometry

24 hours post-transfection, COP5-EBNA cells expressing MAGE-A10 constructs were collected for analyzing the living cells. The cells were washed with PBS and detached from the plate with 1 ml of PBS-EDTA reagents. Then, the cells were centrifuged in a tabletop centrifuge at 4000 rpm at room temperature for 5 minutes and resuspended in 1ml of PBS. The cell samples were analyzed with Attune NxT Acoustic Focusing Cytometer (Invitrogen, Thermo Fisher Scientific). Data analysis was conducted in M.S. Excel.

3.1.6 Western blot analysis

24 hours post-transfection, the cells were washed with PBS and transferred from the cell culture plate to a microcentrifuge tube with 1ml of PBS-EDTA. Then, the cells were centrifuged in a tabletop centrifuge at 4000 rpm at room temperature for 5 minutes and resuspended in 1ml of PBS. Cell lysates were made with 2X Laemmli buffer and boiled for 10 minutes at 100º C. The samples were separated by SDS (sodium dodecyl sulphate)-PAGE (polyacrylamide gel electrophoresis) using a 12% polyacrylamide gel. 15 µl of cell lysates were loaded in each well of the polyacrylamide gel and run initially at 100V using SDS running buffer (125 mM Tris, 960 mM glycine, 0.5% SDS). After the protein samples reached the separating gel, the voltage was raised to 150V.

Proteins were transferred from the gel to a PVDF (polyvinylidene fluoride) membrane (Amersham™ Hybond ™ P 0.45 PVDF blotting membrane, G.E. Healthcare Lifescience) by semi-dry transfer method using TransBlot® SD Semi-Dry Transfer Cell (BioRad) at 15V. The transfer time depended on the number of gels, 20 minutes for 1 gel, 30 minutes for 2 gels, and 45 minutes for 3-4 gels. After transfer, the membrane was blocked in a blocking solution (100 mM Tris, pH 7.5, 170 mM NaCl, TBS-0.05% Tween20, 5% NFDM (non-fat dry milk)) for 30 minutes at room temperature on a shaker.

Specific antibodies were used to detect the proteins. The membranes were incubated in primary antibody solution (100 mM Tris, pH 7.5, 170 mM NaCl, 0.05% Tween20, 2% NFDM (non-fat dry milk)) at 4º C overnight on a shaker. The used primary antibodies and appropriate concentrations are shown in **Table 1**. After incubating with primary antibodies, the membranes were washed three times for 10 minutes using Western blot washing buffer (100 mM Tris, pH 7.5, 170 mM NaCl, 0.05% Tween20) on a shaker. Then, the membranes were incubated in HRP (horseradish peroxidase)-conjugated secondary antibody solution (100 mM Tris, pH 7.5, 170 mM NaCl, 0.05% Tween20, 2% NFDM (non-fat dry milk) for 45 minutes at room temperature on a shaker. The used secondary antibodies and appropriate concentrations are shown in **Table 2**. Then the membranes were washed three times for 10 minutes using Western blot washing buffer (100 mM Tris, pH 7.5, 170 mM NaCl, 0.05% Tween20) on a shaker.

Finally, the protein signals were visualized using Amersham™ ECL (electrochemiluminescence)™ Western Blotting Detection Reagents (G.E. Healthcare Life Science) and exposed onto Agfa X-ray film. The images from the X-ray film were scanned using EPSON EXPRESSION 1680 PRO scanner (Suva, Japan).

3.1.7 Immunofluorescence

COP5-EBNA cells transfected with expression plasmids were grown on cover glasses (12 mm) placed in a 24-well cell culture plate (CellStar®). 24 hours post-transfection, the cover glasses were washed with 1xPBS 3 times for 5 minutes. Then, the cover glasses with cells were fixed with 4% PFA-PBS solution (paraformaldehyde) for 10 minutes at room temperature and permeabilized with 500 µl of 0.2% Triton X-100 in PBS for 10 min while keeping the plate on ice. The cells were washed with 1xPBS 3 times for 5 minutes and blocked in 500 µl of 5% BSA-PBS solution (bovine serum albumin) for 30 minutes. The cells were then incubated with specific primary antibodies, i.e., mouse anti-MAGE-A10 1D12 and mouse

anti-MAGE-A10 4B9 antibodies diluted in 3% BSA-PBS overnight at 4ºC. Following incubation, the cells were washed gently with 1xPBS 3 times for 5 min and then incubated with anti-mouse Alexa Fluor 568 conjugated secondary antibody (**Table 2)** (Invitrogen) for 45 minutes at room temperature. Then, the cover glasses were washed with 1xPBS for 3x5 minutes. The glasses were mounted onto microscope slides using 4 µl of Slow Fade® Gold Antifade reagent with DAPI (6-diamidino-2-phenylindole, Invitrogen). The cells were observed with an LSM710 confocal laser scanning microscope (Zeiss), and the images were obtained using ZEN2011 software (Carl Zeiss AG).

3.2 RESULTS

3.2.1 Size and expression of the MAGE-A10 protein

In order to determine, which stretch of amino acid residues is responsible for the size discrepancy of the MAGE-A10 protein, mouse fibroblast COP5-EBNA cells were transfected with pQM plasmids encoding for different stretches of the MAGE-A10 protein fused with EGFP. A scheme of the MAGE-A10 deletion mutants can be seen in **Figure 4**. The putative molecular weight of the fusion proteins was calculated by using Compute pI/Mw tool (Expasy, Swiss Institute of Bioinformatics) at https://web.expasy.org/compute_pi/ (Bjellqvist et al., 1994). The list of expressed proteins with their lengths and their putative molecular weights is given below in **Table 3**.

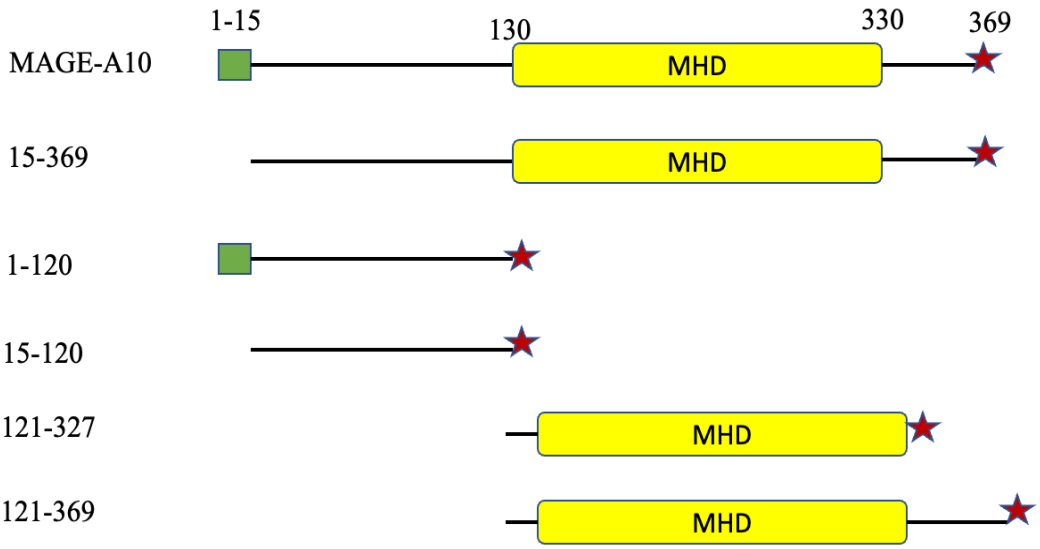

Figure 4. MAGE-A10 deletion mutants. Scheme of MAGE-A10 deletion mutants fused with EGFP (represented with a red star). The conserved MAGE homology domain (MHD) is highlighted in yellow.

Table 3: MAGE-A10 deletion mutant protein characteristics.

Protein name	Length (aa)	Putative molecular weight (kDa)
wt MAGE-A10-EGFP	611	67.9
MAGE-A10$_{1-14}$-EGFP	270	30.4
MAGE-A10$_{15-369}$-EGFP	598	66.4
MAGE-A10$_{1-120}$-EGFP	361	39.5
MAGE-A10$_{15-120}$-EGFP	348	37.9
MAGE-A10$_{121-327}$-EGFP	449	50.9
MAGE-A10$_{121-369}$-EGFP	492	55.7

To determine the size of MAGE-A10 prot2ein, western blot assays were performed (**Figure 5**). Primary antibodies against MAGE-A10 and GFP were used to detect the proteins. Our MAGE-A10-specific antibody does not recognize MAGE- A10$_{1-14}$-EGFP and, therefore, could only be detected only with anti-GFP. Anti-alfa-tubulin was used to determine the quantity of cells in the samples. **Figure 5 (c)** confirms that the quantity of cells was similar in all the samples. Salmon sperm carrier DNA and pure EGFP were used as negative controls in all the experiments. MAGE-A10 is 369 amino acids long (Meek & Marcar, 2012). The deletion mutants used in this study represent both the N-terminal (1 - 14, 1 - 120, 15 - 120) and C-terminal (121 - 327, 121 - 369) regions of the MAGE-A10 protein, whereas MAGE-A10$_{15-369}$-EGFP only differs from the full-length protein by the deletion of the first 14 amino acid residues from the N-terminus.

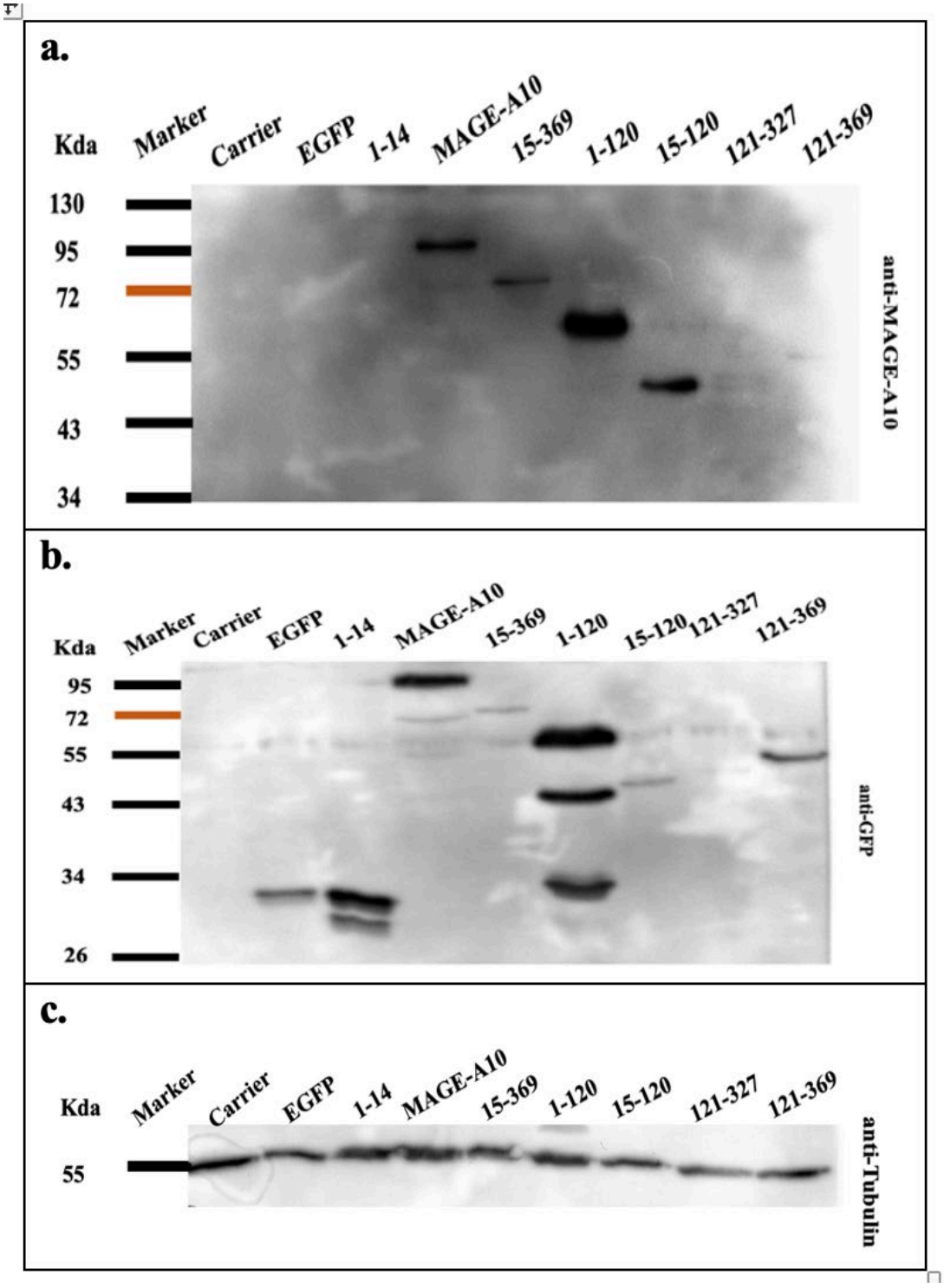

Figure 5. Western blot analysis of the transfected COP5-EBNA cell line with anti-MAGE-A10, anti-GFP, and anti-tubulin antibodies. (**a**) anti-MAGE-A10 was used against MAGE-A10 stretches. The N-terminal regions of the protein showed a higher expression and a shift in size compared to the computational values, whereas the C-terminal regions showed weaker expressions than N-terminus with no size shifts. (**b**) anti-GFP antibody was used to validate the results obtained with anti-MAGE-A10, and similar results as in (**a**) were observed, adding results for EGFP and 1 - 14. Amino acids 1 – 14 did not show any size shift compared to the computational size. (**c**) anti-tubulin antibody used for cellular control represents a similar quantity of cells throughout the samples.

The obtained immunoblotting results show that the regions of the MAGE-A10 protein containing the N-terminal half (1 - 120, 15 - 120, 15 - 369) run higher in the SDS gel and appear to be larger than their computational sizes suggest, whereas the mutants lacking the N-terminal half (121 - 327, 121 - 369) run at their computational sizes **(Figure 5 (a, b)).** However, it can be seen that MAGE-A10$_{1-14}$-EGFP also ran at its computational size, albeit being a part of the N-terminal region **(Figure 5 (b)).** This might be due to the fact that 14 amino acid residues make up a fairly small peptide, and therefore its effects, if there are any, can be overshadowed by GFP and rendered undetectable.

Also, it is visible that the constructs containing the first 14 amino acid residues (1 - 14, 1 - 120) have higher expression rates than those that lack this part (15 - 120, 15 - 369, 121 - 327, 121 - 369) (**Figure 5 (a, b)).** Whether these differences are due to the higher stability or more rigorous production of the N-terminal regions remains to be determined. The obtained results were similar, regardless of the antibody used.

To further confirm the differing expression levels of the different regions of the MAGE-A10 protein, flow cytometry analyses with the transfected cells were performed. The average results of three separate experiments are shown below in **Figure 6**. The observed results corresponded with the previous immunoblotting results, showing that the regions containing the first 14 amino acid residues (1 - 14, 1 -120) have higher expression rates than the constructs that do not contain this stretch (15 - 369, 121 - 327, 121 - 369). Interestingly, MAGE-A10$_{15-120}$-EGFP also has a higher expression rate than the full-length MAGE-A10 protein, like the other N-terminal regions, but its expression is still lower than MAGE-A10$_{1-120}$-EGFP, which contains the first 14 amino acid residues. This confirms that amino acid residues 1 - 14 are critical in the expression of the MAGE-A10 protein, but other parts of the N-terminal half of the protein may also play a role. More specific information is yet to be determined.

Therefore, we can conclude that there is a lower protein expression in the absence of the N-terminal region of the protein, which affects either the stabilization or production of the MAGE-A10 protein.

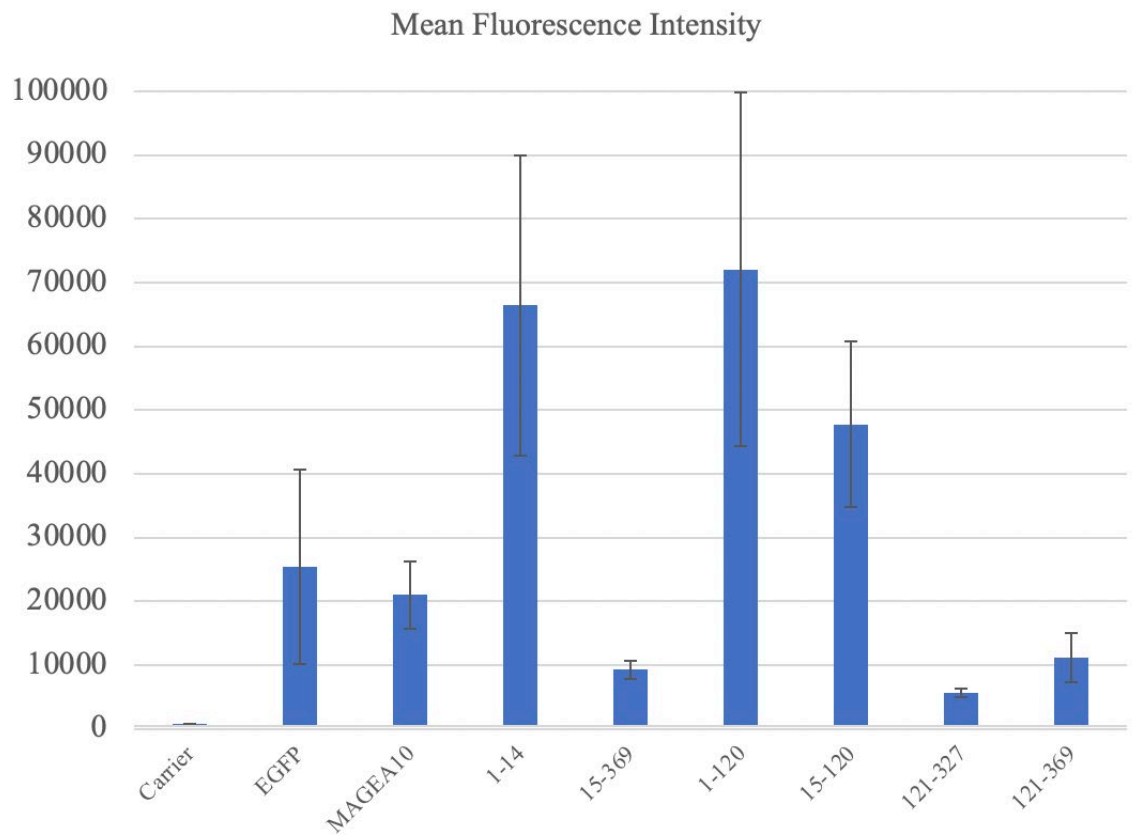

Figure 6. Bar chart of the mean fluorescence intensity values. The data shown in the figure were obtained from the average of three independent experiments. Carrier and EGFP were used as negative controls. 1 - 14, 1 - 120, 15 - 120 showed a higher expression than the full-length protein MAGE-A10, whereas 15 - 369, 121 - 327, and 121 - 369 showed lower expression levels. Error bars indicate standard errors.

3.2.2 Localization of the MAGE-A10 protein

An immunofluorescence assay was performed to determine the localization of the MAGE-A10 protein deletion mutants in mouse fibroblast cells. In-house specific monoclonal antibodies to MAGE-A10, i.e., anti-MAGE-A10 1D12 and anti-MAGE-A10 4B9, were used to study the localization of the mutants within the cells. The anti-MAGE-A10 1D12 antibody recognizes a stretch of amino acids in the C-terminal region, thus detecting the full-length MAGE-A10 and mutants 15 - 369, 121 - 327, 121 - 369. Anti-MAGE-A10 4B9 recognizes a stretch of amino acids in the N-terminal region and was used to detect the full-length MAGE-A10 and mutants 15 - 369, 1 - 120, and 15 - 120. Pure EGFP and carrier DNA were used as negative controls. Unfortunately, MAGE-A10$_{1\text{-}14}$-EGFP could not be detected with either antibody. With anti-MAGE-A10 4B9, the antibody gives either a cross-reaction with GFP or a general background signal, which can be seen in the cytoplasm of the cell, sometimes concentrated into cytoplasmic foci.

The full-length MAGE-A10-EGFP protein was mainly detected in the nucleus of the cell (**Figure 7, 8**), which correlates with the previous studies (Carrel et al., 1996). A similar result was obtained by observing the GFP signal of MAGE-A10$_{1\text{-}14}$-EGFP, which was mainly present in the cell nucleus (**Figure 7, 8**). However, some cytoplasmic localization was also seen, which might be the influence of GFP since GFP alone localizes all over the cell. MAGE-A10$_{15\text{-}369}$-EGFP, which differs from the full-length protein by the deletion of the first 14 amino acid residues, was only detected in the cytoplasm of the cell with both monoclonal antibodies (**Figure 7, 8**). Similarly, the C-terminal regions of MAGE-A10 (121 - 327, 121 - 369) were shown to be localized in the cytoplasm of the cell (**Figure 7**). However, the GFP signal of these mutants displayed the localization in both the nucleus and cytoplasm of the mouse fibroblast cells. This could be due to the influence of GFP in the fusion protein since GFP by itself is localized all over the cell, including in the nucleus.

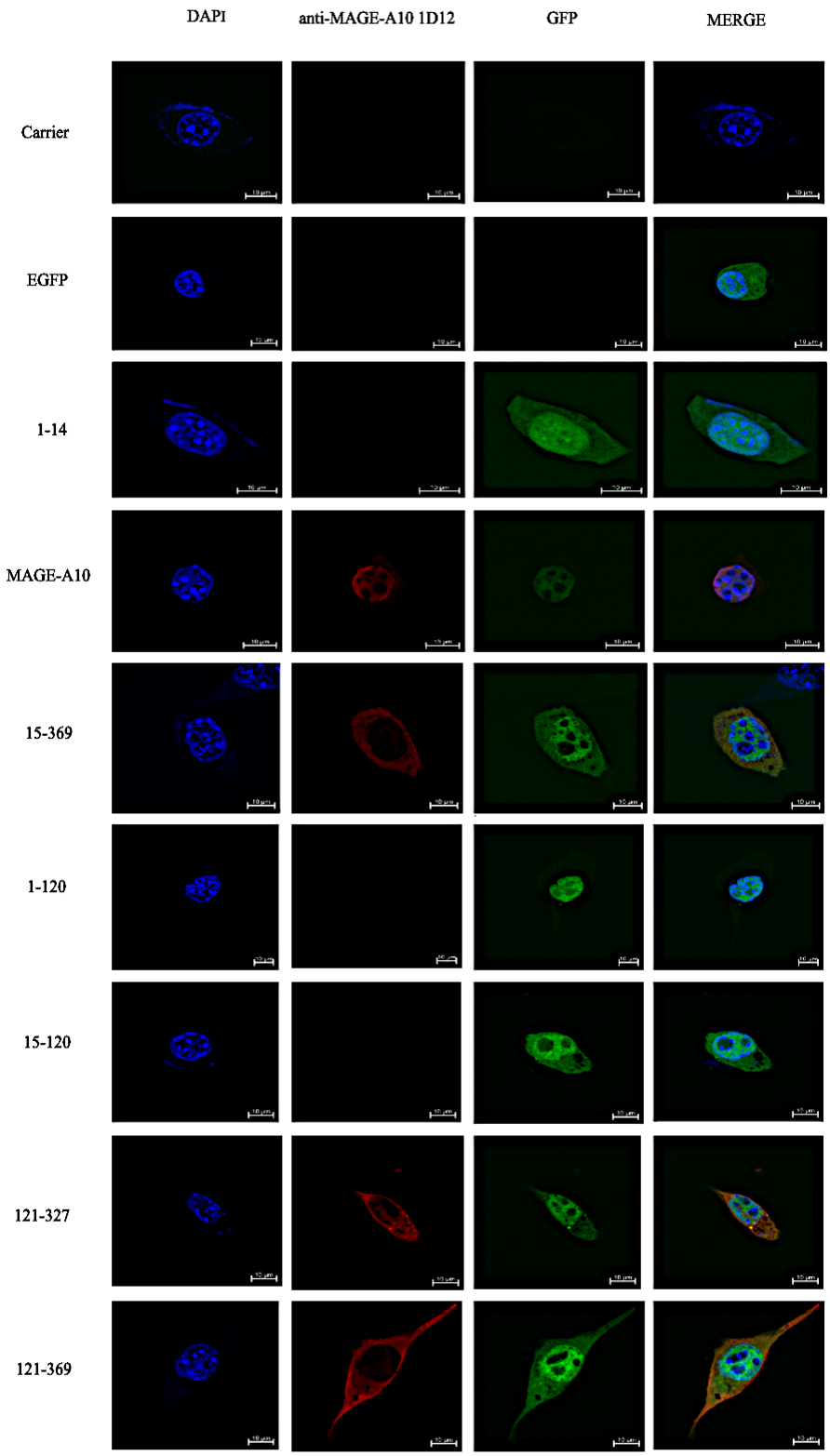

Figure 7. Expression of MAGE-A10 protein in COP5-EBNA cells. The COP5-EBNA cells transfected with plasmids encoding for the EGFP fusion proteins of MAGE-A10 deletion mutants were grown on coverslips, fixed, and incubated with a specific monoclonal antibody against MAGE-A10, i.e., anti-MAGE-A10 1D12 and visualized with Alexa568-conjugated secondary antibody (red). Cell nuclei were stained with DAPI.
Scale bar = 10μm.

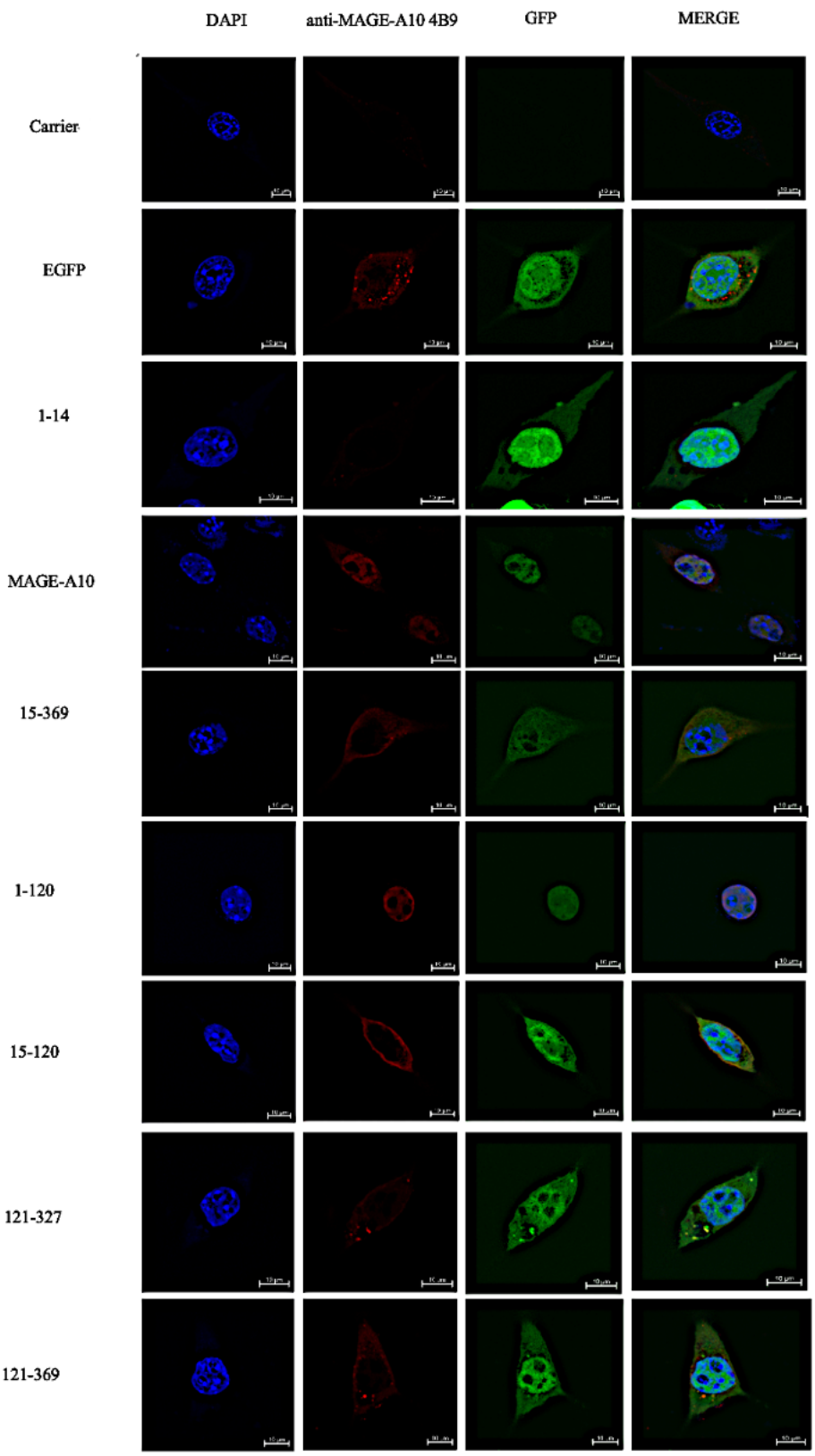

Figure 8. Expression of MAGE-A10 protein in COP5-EBNA cells. The COP5-EBNA cells transfected with plasmids encoding for the EGFP fusion proteins of MAGE-A10 deletion mutants were grown on coverslips, fixed, and incubated with a specific monoclonal antibody against MAGE-A10, i.e., anti-MAGE-A10 4B9 and visualized with Alexa568-conjugated secondary antibody (red). Cell nuclei were stained with DAPI.
Scale bar = 10μm.

MAGE-A10$_{1\text{-}120}$-EGFP was also observed in the cell's nucleus, similar to the full-length protein and MAGE-A10$_{1\text{-}14}$-EGFP **(Figure 8).** Both the antibody and the GFP signals displayed the localization in the nucleus. However, MAGE-A10$_{15\text{-}369}$-EGFP, which lacks the first 14 amino acid residues, was observed in the cytoplasm of the cell and not in the nucleus when looking at the antibody signal (**Figure 8**). The differences between antibody and GFP signals may be due to GFP influence on the fusion proteins since GFP by itself can be found all over the cell. Similarly, the MAGE-A10$_{15\text{-}120}$-EGFP was also observed in the cytoplasm of the cell (**Figure 8**).

Therefore, our data suggest that the first 14 amino acid residues are responsible for nuclear localization. In the absence of these residues, the proteins are mainly localized in the cell's cytoplasm.

3.3 DISCUSSION

During this work, the melanoma antigen MAGE-A10 was studied, paying special attention to its size discrepancy and nuclear localization. MAGE-A10 protein is predominantly expressed in lung cancers, squamous cell carcinomas, adenocarcinomas, large and small cell cancers, and to some extent in several other cancers. Furthermore, high expression of MAGE-A10 has been detected at the protein level in the stomach, gall bladder, and gynecological malignancies (Schultz-Thater et al., 2010). MAGE-A10 protein is one of the most antigenic members of the MAGE family and is, therefore, a potential target for cancer immunotherapy and cancer vaccines (Schultz-Thater et al., 2010). The further characterization of MAGE-A10 protein might set a significant step towards developing targeted active immunotherapy. Previous studies have shown that MAGE-A10 is a nuclear protein (Carrel et al., 1996). As suggested by computational values, the protein is about ~41kDa but runs at ~72kDa in the gel. However, the potential reason for this size anomaly of MAGE-A10 had not been studied.

In order to further study the MAGE-A10, the present study has examined which stretch of amino acid residues might be responsible for the size discrepancy and the nuclear localization of the protein.

Western blot analyses were performed to determine the sizes of different regions of the MAGE-A10 protein. The sample of plasmid transfected cells showed that the regions of the MAGE-A10 protein containing the N-terminal half (1 - 120, 15 - 120, 15 - 369) ran higher in the SDS gel and appeared to be larger than their computational sizes suggest. Also, the constructs containing the first 14 amino acid residues (1 -14, 1 - 120) showed a higher expression than those lacking this part (15 - 120, 15 - 369, 121 - 327, 121 - 369). It is possible that there might be protein modifications in the N-terminal region of the MAGE-A10 protein, which might have resulted in the size anomalies of the MAGE-A10 protein. Another possibility could be that those samples might not have been adequately denatured before running them in the SDS gel, which could have resulted in unfolded secondary structures. This, however, requires further investigation.

Flow cytometry was performed to confirm the different expression levels of the different regions of the MAGE-A10 protein. The results were similar to that of the western blot analyses, where the first 14 amino acid residues (1 - 14, 1 - 120) showed higher expression rates than the constructs that do not contain this stretch (15 - 120, 15 - 369, 121 - 327, 121 - 369).

Whether these differences in expression levels are due to the higher stability or more rigorous production of the constructs containing the short N-terminal region remains to be determined. It was also observed that the N-terminal region lacking the first 14 amino acid residues (15 - 120) showed a higher expression rate than the full-length protein or the C-terminal regions but a lower expression rate than that of MAGE-A10$_{1-120}$-EGFP. Therefore, it is still unknown whether only the first 14 amino acids or other parts of the N-terminal half of the protein play roles in determining the expression level.

During immunofluorescence studies, the localization of MAGE-A10 protein was studied. In-house specific monoclonal antibodies to MAGE-A10 stretches were used. As previous studies suggested (Carrel et al., 1996), the full-length MAGE-A10-EGFP protein was localized mainly in the nucleus of the cell. Similarly, the first bit of the protein, i.e., MAGE-A10$_{1-14}$-EGFP, also localized mainly in the cell nucleus, but showed some cytoplasmic localization as well, which could be the influence of GFP since GFP alone localizes all over the cell. The N-terminal MAGE-A10$_{1-120}$-EGFP was observed in the cell's nucleus with both antibodies and the GFP signal. The deletion mutants (1 - 14 and 1 - 120) containing the first 14 amino acid residues were localized in the nucleus, whereas constructs MAGE-A10$_{15-120}$-EGFP and MAGE-A10$_{15-369}$-EGFP, which lack the first 14 amino acid residues, were detected in the cytoplasm of the cell. Differences were observed when looking at the antibody and GFP signal. These differences between antibody and GFP signals may be due to GFP influence on the fusion proteins. The possible reason for the nuclear localization could be that there might be an NLS (nuclear localization signal) in these N-terminal regions (1 - 14 and 1 - 120) responsible for nuclear localization. However, it is yet to be discovered which of the amino acid residues is exactly showing this NLS. Adding to this, the type of the NLS is also unknown, and further study has to be done to understand more about the protein's localization.

The C-terminal regions of MAGE-A10 (121 - 327, 121 - 369) localized in the cytoplasm of the cell. However, the GFP signal of these mutants also displayed the localization in both the nucleus and cytoplasm of the mouse fibroblast cells, similar to that of MAGE-A10$_{15-369}$-EGFP. This might be due to the influence of GFP in the fusion protein since GFP by itself is localized all over the cell, including in the nucleus.

Our data suggest that the first 14 amino acid residues are responsible for the higher expression of MAGE-A10 protein and nuclear localization, because in the absence of these resi-

dues, the proteins showed lower expression and were mainly localized in the cell's cytoplasm. There are still many questions about how these amino acids influence the protein's characteristics. Moreover, further research is needed to understand the MAGE-A10 protein in depth, to successfully use it for targeted active immunotherapy in the future.

SUMMARY

The aim of the present thesis was to find out which stretch of amino acid residues is responsible for the size anomalies and nuclear localization of the MAGE-A10 protein. Eukaryotic COP5-EBNA cells were transfected with in-house pQM plasmids expressing MAGE-A10 proteins.

The experiments revealed that the first 14 amino acid residues are critical in the expression of MAGE-A10 protein. It was shown that the regions of the MAGE-A10 protein containing the N-terminal half ran higher in the SDS gel and appeared to be larger than their computational sizes suggested, whereas the mutants lacking the N-terminal half ran at their computational sizes. Furthermore, the flow cytometry results showed that the regions containing the first 14 amino acid residues had higher expression rates than the constructs that do not contain this stretch. Therefore, we can conclude that there is a lower protein expression in the absence of the first 14 amino acid residues, and these differences in the expression levels might occur due to the higher stability or more rigorous production of the N-terminal regions. What exactly causes the size differences in the N-terminal region of the protein, remained unsolved and needs further research.

This study also showed that the first 14 amino acid residues are responsible for the nuclear localization of MAGE-A10. In the absence of these amino acid residues, the protein had cytoplasmic localization. Further information about potential nuclear localization signals and pathways was not a part of this study and remains to be determined.

REFERENCES

Atanackovic, D., Altorki, N. K., Stockert, E., Williamson, B., Jungbluth, A. A., Ritter, E., Santiago, D., Ferrara, C. A., Matsuo, M., Selvakumar, A., Dupont, B., Chen, Y.-T., Hoffman, E. W., Ritter, G., Old, L. J., & Gnjatic, S. (2004). Vaccine-Induced CD4 + T Cell Responses to MAGE-3 Protein in Lung Cancer Patients. The Journal of Immunology, 172(5), 3289–3296. https://doi.org/10.4049/jimmunol.172.5.3289

Barker, P. A., & Salehi, A. (2002). Mini-Review The MAGE Proteins: Emerging Roles in Cell Cycle Progression, Apoptosis, and Neurogenetic Disease. https://doi.org/10.1002/jnr.10160

Becker', Jurgen C, Gillitzer, R., & Brocker, E.-B. (1994). A member of the melanoma antigen-encoding gene (MAGE) family is expressed in human skin during wound healing. In Int. J. Cancer (Vol. 58).

Bjellqvist, B., Basse, B., Olsen, E. and Celis, J.E. Reference points for comparisons of two-dimensional maps of proteins from different human cell types defined in a pH scale where isoelectric points correlate with polypeptide compositions. Electrophoresis 1994, 15, 529-539.

Caballero, O. L., & Chen, Y.-T. (2009). Cancer/testis (C.T.) antigens: Potential targets for immunotherapy. https://doi.org/10.1111/j.1349-7006.2009.01303.x

Cancer Research Institute, (2022a), Cancer treatment types, Available at: https://www.cancerresearch.org/immunotherapy/treatment-types (Last accessed on 20.04.22 at 13:00)

Cancer Research Institute, (2022b), Immunotherapy, Available at: https://www.cancerresearch.org/en-us/immunotherapy/why-immunotherapy (Last accessed on 20.04.22 at 14:00)

Carrel, S., Schreyer', M., Spagnoli', G., Ceroitini~, J.-C., & Rimoldi', D. (1996). Monoclonal antibodies against recombinant-MAGE-1 protein identify a cross-reacting 72-kDa antigen which is co-expressed with MAGE-1 protein in melanoma cells. In Int. J. Cancer (Vol. 67). Wiley-Liss, Inc.

Chang, Y., Wang, X., Xu, Y., Yang, L., Qian, Q., Ju, S., Chen, Y., Chen, S., Qin, N., Ma, Z., Dai, J., Ma, H., Jin, G., Zhang, E., Wang, C., Hu, Z., & Zhibin Hu, C. (2019). Comprehensive characterization of cancer-testis genes in testicular germ cell tumor. Cancer Medicine, 8, 3511–3519. https://doi.org/10.1002/cam4.2223

Chomez, P., de Backer, O., Bertrand, M., de Plaen, E., Boon, T., & Lucas, S. (2001). An Overview of the MAGE Gene Family with the Identification of All Human Members of the Family. 1. In CANCER RESEARCH (Vol. 61). http://aacrjournals.org/cancerres/article-pdf/61/14/5544/2862930/ch140105544.pdf

Colemon, A., Harris, T. M., & Ramanathan, S. (2020). DNA hypomethylation drives changes in MAGE-A gene expression resulting in alteration of proliferative status of cells**.** Genes and Environment, 42(1). https://doi.org/10.1186/s41021-020-00162-2

de Donato, M., Peters, S. O., Hussain, · Tanveer, Rodulfo, H., Thomas, B. N., Masroor, ·, & Babar, E. (2017). Molecular evolution of type II MAGE genes from ancestral MAGED2 gene and their phylogenetic resolution of basal mammalian clades. Mammalian Genome, 28, 443–454. https://doi.org/10.1007/s00335-017-9695-6

de Plaen, E., Karen, •, Catia, A. •, Jos6, T., Gaforio, J., Szikora, J.-P., de Smet, C., Brasseur, F., van der Bruggen, P., Leth6, B., Lurquin, C., Brasseur, R., Chomez, P., de Backer, O., Cavenee, W., Boon, T., Arden, K., Cavenee, • W, & Brasseur, R. (1994). Structure, chromosomal localization, and expression of 12 genes of the MAGE family. In Immunogenetics (Vol. 40).

Doyle, J. M., Gao, J., Wang, J., Yang, M., & Potts, P. R. (2010). MAGE-RING protein complexes comprise a family of E3 ubiquitin ligases. Molecular Cell, 39(6), 963–974. https://doi.org/10.1016/j.molcel.2010.08.029

Duperret, E. K., Liu, S., Paik, M., Trautz, A., Stoltz, R., Liu, X., Ze, K., Perales-Puchalt, A., Reed, C., Yan, J., Xu, X., & Weiner, D. B. (2018). Translational Cancer Mechanisms and Therapy A Designer Cross-reactive DNA Immunotherapeutic Vaccine that Targets Multiple MAGE-A Family Members Simultaneously for Cancer Therapy. https://doi.org/10.1158/1078-0432.CCR-18-1013

Forslund, K. Ö., & Nordqvist, K. (2001). The melanoma antigen genes - Any clues to their functions in normal tissues? In Experimental Cell Research (Vol. 265, Issue 2, pp. 185–194). Academic Press Inc. https://doi.org/10.1006/excr.2001.5173

Gonzaga Almeida, L., Sakabe, N. J., Deoliveira, A. R., Cristina, M., Silva, C., Mundstein, A. S., Cohen, T., Chen, Y.-T., Chua, R., Gurung, S., Gnjatic, S., Jungbluth, A. A., Via, O., Caballero, L., Bairoch, A., Kiesler, E., White, S. L., Simpson, A. J. G., Old, L. J., … Vasconcelos, R. (2009). C.T. database: a knowledge-base of high-throughput and

curated data on cancer-testis antigens. Nucleic Acids Research, 37. https://doi.org/10.1093/nar/gkn673

Jurk, M., Kremmer, E., Schwarz, U., Fo¨rster, R., Fo¨rster, F., & Winnacker, E.-L. (1998). MAGE-11 protein is highly conserved in higher organisms and located predominantly in the nucleus.

Kozakova, L., Vondrova, L., Stejskal, K., Charalabous, P., Kolesar, P., Lehmann, A. R., Uldrijan, S., Sanderson, C. M., Zdrahal, Z., & Palecek, J. J. (2015). Cell Cycle The melanoma-associated antigen 1 (MAGEA1) protein stimulates the E3 ubiquitin-ligase activity of TRIM31 within a TRIM31-MAGEA1-NSE4. https://doi.org/10.1080/15384101.2014.1000112

Kulkarni, P., Uversky, V. N., & Stephan, C. (2017). Cancer/Testis Antigens: "Smart" Biomarkers for Diagnosis and Prognosis of Prostate and Other Cancers. International Journal of Molecular Sciences Article. https://doi.org/10.3390/ijms18040740

Kurg, R., Reinsalu, O., Jagur, S., Õunap, K., Võsa, L., Kasvandik, S., Padari, K., Gildemann, K., & Ustav, M. (2016). Biochemical and proteomic characterization of retrovirus Gag based microparticles carrying melanoma antigens OPEN. https://doi.org/10.1038/srep29425

Laduron, S., Deplus, R., Zhou, S., Kholmanskikh, O., le Godelaine, D., de Smet, C., Hayward, S. D., Ois Fuks, F., Boon, T., & de Plaen, E. (2004). MAGE-A1 interacts with adaptor SKIP and the deacetylase HDAC1 to repress transcription. https://doi.org/10.1093/nar/gkh735

Lee, A. K., & Potts, P. R. (2017). A Comprehensive Guide to the MAGE Family of Ubiquitin Ligases. In Journal of Molecular Biology (Vol. 429, Issue 8, pp. 1114–1142). Academic Press. https://doi.org/10.1016/j.jmb.2017.03.005

Lipkowitz, S., & Weissman, A. M. (2011). RINGs of good and evil: RING finger ubiquitin ligases at the crossroads of tumour suppression and oncogenesis. https://doi.org/10.1038/nrc3120

Lira Da Silva, V., Fonseca, A. F., Fonseca, M., Emilia Da Silva, T., Coelho, A. C., Kroll, J. E., Santana De Souza, J. E., Stransky, B., Antonio De Souza, G., & José De Souza, S. (2017). Genome-wide identification of cancer/testis genes and their association with prognosis in a pan-cancer analysis. www.impactjournals.com/oncotarget

Liu, S., Zhao, Y., Xu, Y., Sang, M., Zhao, R., Gu, L., & Shan, B. (2020). The clinical significance of methylation of MAGE-A1 and-A3 promoters and expression of DNA methyltransferase in patients with laryngeal squamous cell carcinoma. American Journal of Otolaryngology - Head and Neck Medicine and Surgery, 41(1). https://doi.org/10.1016/j.amjoto.2019.102318

Liu, Y., Wen, L., Ma, L., Kang, Y., Liu, K.-Y., Huang, X.-J., Ruan, G.-R., & Lu, J. (2019). MAGE genes: Prognostic indicators in A.L. amyloidosis patients. J Cell Mol Med, 23. https://doi.org/10.1111/jcmm.14475

Liu, Y., Yang, S., Yang, J., Que, H., & Liu, S. (2012). Relative Expression of Type II MAGE Genes During Retinoic Acid-Induced Neural Differentiation of Mouse Embryonic Carcinoma P19 Cells: A Comparative Real-Time PCR Analysis. https://doi.org/10.1007/s10571-012-9826-2

López-Sánchez, N., González-Fernández, Z., Niinobe, M., Yoshikawa, K., & Frade, J. M. (2007). Single mage gene in the chicken genome encodes CMage, a protein with functional similarities to mammalian type II Mage proteins. Physiol Genomics, 30, 156–171. https://doi.org/10.1152/physiolgenomics.00249.2006.-In

Lorick, K. L., Jensen, J. P., Fang, S., Ong, A. M., Hatakeyama, S., & Weissman, A. M. (1999). RING fingers mediate ubiquitin-conjugating enzyme (E2)-dependent ubiquitination. In National Institutes of Health (Vol. 96). www.pnas.org.

Lucas, S., de Smet, C., Arden, K. C., Viars, C. S., Lethã©, B., Lurquin, C., & Boon, T. (1998). Identification of a New MAGE Gene with Tumor-specific Expression by Representational Difference Analysis. In CANCER RESEARCH (Vol. 58). http://aacrjournals.org/cancerres/article-pdf/58/4/743/2468771/cr0580040743.pdf

Makise, N., Morikawa, T., Nakagawa, T., Ichimura, T., Kawai, T., Matsushita, H., Kakimi, K., Kume, H., Homma, Y., & Fukayama, M. (2016). MAGE-A expression, immune microenvironment, and prognosis in upper urinary tract carcinoma. Human Pathology, 50, 62–69. https://doi.org/10.1016/j.humpath.2015.11.007

Meek, D. W., & Marcar, L. (2012). MAGE-A antigens as targets in tumour therapy. In Cancer Letters (Vol. 324, Issue 2, pp. 126–132). Elsevier Ireland Ltd. https://doi.org/10.1016/j.canlet.2012.05.011

Monte, M., Simonatto, M., Peche, L. Y., Bublik, D. R., Gobessi, S., Pierotti, M. A., Rodolfo, M., & Schneider, C. (2006). MAGE-A tumor antigens target p53 transactivation function through histone deacetylase recruitment and confer resistance to chemotherapeutic agents. www.pnas.orgcgidoi10.1073pnas.0510834103

Muscatelli, F., Walker, A. P., de Plaent, E., Stafford, A. N., Monaco, A. P., & Ludwig, *. (1995). Isolation and characterization of a MAGE gene family in the Xp21.3 region (X chromosome/dosage-sensitive sex reversal locus). In Genetics (Vol. 92).

Pineda, C. T., Ramanathan, S., Fon Tacer, K., Weon, J. L., Potts, M. B., Ou, Y. H., White, M. A., & Potts, P. R. (2015). Degradation of AMPK by a Cancer-Specific Ubiquitin Ligase. Cell, 160(4), 715–728. https://doi.org/10.1016/J.CELL.2015.01.034

Rimoldi, D., Salvi, S., Reed, D., Coulie, P., Jongeneel, V. C., de Plaen, E., Brasseur, F., Rodriguez, A.-M., Boon, T., & Cerottini, J.-C. (1999). cDNA and protein Characterization of human MAGE-10.

Rogner, U. C., Wilke, K., Steck, E., Korn, B., & Poustka, A. (1995). The Melanoma Antigen Gene (MAGE) Family Is Clustered in the Chromosomal Band Xq28. In GENOMICS (Vol. 29).

Saito, T., Wada, H., Yamasaki, M., Miyata, H., Nishikawa, H., Sato, E., Kageyama, S., Shiku, H., Mori, M., & Doki, Y. (2014). High expression of MAGE-A4 and MHC class I antigens in tumor cells and induction of MAGE-A4 immune responses are prognostic markers of CHP-MAGE-A4 cancer vaccine. Vaccine, 32(45), 5901–5907. https://doi.org/10.1016/j.vaccine.2014.09.002

Schultz-Thater, E., Piscuoglio, S., Iezzi, G., le Magnen, C., Zajac, P., Carafa, V., Terracciano, L., Tornillo, L., & Spagnoli, G. C. (2010). MAGE-A10 is a nuclear protein frequently expressed in high percentages of tumor cells in lung, skin, and urothelial malignancies. https://doi.org/10.1002/ijc.25777

Shichijo, S., Tsunosue, R., Kubo, K., Kuramoto, T., Tanaka, Y., Hayashi', A., & Itoh, K. (1995). Establishment of an enzyme-linked immunosorbent assay (ELISA) for measuring cellular MAGE-4 protein on human cancers. In Journal of Immunological Methods (Vol. 186). ELSEVIER.

Suzuki, S., Sasajima, K., Sato, Y., Watanabe, H., Matsutani, T., Iida, S., Hosone, M., Tsukui, T., Maeda, S., Shimizu, K., & Tajiri, T. (2008). MAGE-A protein and MAGE-A10

gene expressions in liver metastasis in patients with stomach cancer. British Journal of Cancer, 99, 350–356. https://doi.org/10.1038/sj.bjc.6604476

Taguchi, A., Taylor, A. D., Rodriguez, J., Liu, H., Ma, X., Zhang, Q., Wong, C.-H., Chin, A., Girard, L., Behrens, C., Lam, W. L., Lam, S., Minna, J. D., Wistuba, I. I., Gazdar, A. F., & Hanash, S. M. (2014). A Search for Novel Cancer/Testis Antigens in Lung Cancer Identifies VCX/Y Genes, Expanding the Repertoire of Potential Immunotherapeutic Targets. https://doi.org/10.1158/0008-5472.CAN-13-3725

Töhönen, V., Forslund, hman, & Nordqvist, K. (2000). Mage-b4, a Novel Melanoma Antigen (MAGE) Gene Specifically Expressed during Germ Cell Differentiation 1. In CANCER RESEARCH (Vol. 60). http://aacrjournals.org/cancerres/article-pdf/60/4/1054/2483067/ch040001054.pdf

van der Bruggen, P., Traversari, C., Chomez, P., Lurquin, C., de Plaen, E., Knuth, A., Boont, T., van den Eynde, B., & Boon, T. (1991). A Gene Encoding an Antigen Recognized by Cytolytic T Lymphocytes on a Human Melanoma. https://www.science.org

Vansteenkiste, J., Zielinski, M., Linder, A., Dahabreh, J., Gonzalez, E. E., Malinowski, W., Lopez-Brea, M., Vanakesa, T., Jassem, J., Kalofonos, H., Perdeus, J., Bonnet, R., Basko, J., Janilionis, R., Passlick, B., Treasure, T., Gillet, M., Lehmann, F. F., & Brichard, V. G. (2013). Adjuvant MAGE-A3 immunotherapy in resected non–small-cell lung cancer: Phase II randomized study results. Journal of Clinical Oncology, 31(19), 2396–2403. https://doi.org/10.1200/JCO.2012.43.7103

Warburton, P. E., Giordano, J., Cheung, F., Gelfand, Y., & Benson, G. (2004). Inverted repeat structure of the human genome: The X-chromosome contains a preponderance of large, highly homologous inverted repeated that contain testes genes. Genome Research, 14(10 A), 1861–1869. https://doi.org/10.1101/gr.2542904

Weon, J. L., & Potts, P. R. (2015). The MAGE protein family and cancer. In Current Opinion in Cell Biology (Vol. 37, pp. 1–8). Elsevier Ltd. https://doi.org/10.1016/j.ceb.2015.08.002

World Health Organization (2006), World Cancer Detail. Available at: https://www.who.int/data/mortality/country-profile (Last accessed on 28.04.2022 at 15:00)

World Health Organization, (2022), World Cancer Detail. Available at: https://www.who.int/en/news-room/fact-sheets/detail/cancer (Last accessed on 29.04.2022 at 11:00)

Xiao, T. Z., Bhatia, N., Urrutia, R., Lomberk, G. A., & Simpson, A. (2011). MAGE I Transcription Factors Regulate KAP1 and KRAB Domain Zinc Finger Transcription Factor Mediated Gene Repression. PLoS ONE, 6(8), 23747. https://doi.org/10.1371/journal.pone.0023747

Yang, B., O'herrin, S. M., Wu, J., Reagan-Shaw, S., Ma, Y., Bhat, K. M. R., Gravekamp, C., Setaluri, V., Peters, N., Hoffmann, F. M., Peng, H., Ivanov, A. v, Simpson, A. J. G., & Longley, B. J. (2007). MAGE-A, mMage-b, and MAGE-C Proteins Form Complexes with KAP1 and Suppress p53-Dependent Apoptosis in MAGE-Positive Cell Lines. https://doi.org/10.1158/0008-5472.CAN-07-1478

Yang, P., Meng, M., & Zhou, Q. (2021). Oncogenic cancer/testis antigens are a hallmarker of cancer and a sensible target for cancer immunotherapy. In Biochimica et Biophysica Acta - Reviews on Cancer (Vol. 1876, Issue 1). Elsevier B.V. https://doi.org/10.1016/j.bbcan.2021.188558

NON-EXCLUSIVE LICENCE TO REPRODUCE THESIS AND MAKE THESIS PUBLIC

I, Anjali Gyawali,

1. herewith grant the University of Tartu a free permit (non-exclusive licence) to

reproduce, for the purpose of preservation, including for adding to the DSpace digital archives until the expiry of the term of copyright,

Characterization of Human MAGE-A10 protein,

supervised by Anneli Samel,

2. I grant the University of Tartu a permit to make the work specified in p. 1 available to the public via the web environment of the University of Tartu, including via the DSpace digital archives, under the Creative Commons licence CC BY NC ND 3.0, which allows, by giving appropriate credit to the author, to reproduce, distribute the work and communicate it to the public, and prohibits the creation of derivative works and any commercial use of the work from **1.06.2024** until the expiry of the term of copyright.

3. I am aware of the fact that the author retains the rights specified in p. 1 and 2.

4. I certify that granting the non-exclusive licence does not infringe other persons' intellectual property rights or rights arising from the personal data protection legislation.

Anjali Gyawali

26/05/2022